# Long-Term Effects of Collagen-Binding Mesenchymal Stem Cells Affinity Peptide on Skin Regeneration and Scar Formation Running Title: MSC Capturing Collagen and Skin Regeneration

**Huili Wang**
The Second Affiliated Hospital of Nanjing University of Chinese Medicine
**Xin Yan**
Nanjing University Medical School Affiliated Nanjing Drum Tower Hospital
**Yue Lin**
Nanjing University Medical School Affiliated Nanjing Drum Tower Hospital
**Shuqin Wang**
Nanjing University Medical School Affiliated Nanjing Drum Tower Hospital
**Yanan Jiang**
Nanjing University Medical School Affiliated Nanjing Drum Tower Hospital
**Qian Tan** ( smmmutanqian@sina.com )

**Research article**

**Keywords:** MSCs affinity peptide, Collagen scaffold, Tissue regeneration

**Posted Date:** August 5th, 2020

**DOI:** https://doi.org/10.21203/rs.3.rs-51090/v1

# Abstract

The medical significance of mesenchymal stem cells (MSCs) is not only providing a promising strategy for cutaneous wound healing, but also bringing alternative for the patients whose wounds or burns were difficult to treat and heal. In our previous researches, we produced a fusion protein (Collagen/CBD-E7 peptide) which had high affinity to MSCs and then bound it to collagen scaffold with a CBD (collagen-binding domain). When applied to full-thickness skin defect porcine models, MSCs could be specifically raised to target area which helps accelerate coalescence at early stage. However, scar is an indispensable part of the tissue repair, arising after almost every dermal injury with abnormal appearance and functional disturbance. It usually takes one to three years for the scars to pale and mature. Thus, in this study, we focused on the structure repair of skin defect more than one year after the wounds healing. We found that at the 16w after operation, the proportion of collagen type III was more than collagen type I in Collagen/CBD-E7 peptide group, which indicates a higher healing quality comparatively. While at the 64w, the ratio between collagen type I and collagen type III reached a balance of natural skin tissues. In addition, cutaneous appendages were observed in Collagen/CBD-E7 peptide scaffold group at the 16w and 64w after surgery. From this point of view, the functional collagen scaffold treatments may be able to improve the cosmetic outcome of injury, burns or trauma, and scars are no longer an inevitable consequence of skin healing. This will also imply that humans would no longer be suffering from the scars caused by skin trauma, which is of significant orthopaedic meaning.


# 1. Introduction

Skin, the largest organ of human body, primarily serves as a protective barrier between organism and outer environment [1]. Loss of skin integrity may result in acutely substantial physiologic imbalance and ultimately leads to significant disability or even death [2]. However, failure occurs in different levels as treatments for skin defect still leave much to desire: the availability of healthy skin, the donor-site complication, scar hyperplasia together with the risk of immune rejection are all considered to be obstacles for traditional methods of deep wounds repair such as split-thickness grafts, allogeneic and xenogeneic skin grafts [3]. Thus, in order to overcome the difficulties brought by such limitations, to develop new repair therapy is a matter of great urgency.

In recent years, stem cell therapy has emerged as a potential therapeutic strategy for full-thickness wound repair [4]. Among all types of stem cells, autologous MSCs have become the focus of research due to their unique characteristics of self-renewal, multi-lineage differentiation and low immunogenicity [5, 6]. The MSCs present in bone marrow stromal and the stromal of other organs including placenta, subcutaneous adipose tissue, and muscles [7]. Researches have shown that the cultured autologous MSCs are capable of accelerate the process of the healing of large full-thickness skin wounds in murines, rabbits and humans [8, 9]. However, the application of MSCs therapy was hinderedby inability to target specifically. In our previous study, we produced a functional collagen scaffold which had high specific affinity to MSCs consisting of the MSC-E7 peptide and a collagen-binding domain [10]. When applied in

full-thickness skin defect porcine models, it couldeffectively enhance the recruitment of MSCs, improving blood perfusion and promote wound healing at the 1w、2w、3w、4w weeks [10].

The ideal repair method is to completely regenerate, so that the new tissue may have the same structure as the original uninjured skin. However, scars are the final stage of mammalian tissue repair, and it usually takes one to three years to pale and mature [11]. In this study, we aim to evaluate the functional collagen scaffold in porcine full-thickness skin defect models for a long-term on skin regeneration and scar formation.

# 2. Materials And Methods

### *2.1The CBD-E7 functional collagen scaffolds*

The main material used in the study, collagen scaffold, which is also the focus of this research, was provided by Institute of Genetics and Developmental Biology, Chinese Academy of Sciences (Beijing, China) [10, 12] by synthesizing CBD-E7 peptides (“EPLQLKMGSAGSAAGSGGTKKTLRT”) through solidphase peptide synthesis using Fmoc Chemistry (Scilight-Peptide Inc., Beijing, China), after which 250 μg CBD-E7 peptides were dissolved in 100 μl PBS and added to collagen scaffold.

The scaffold was cut into squares of 5.0×5.0 cm, and the surface morphology both pre-and post-treatment was observed by scanning electron microscopy (SEM) (model S-2500, Hitachi, Japan) (Fig. 1).

### *2.2 Animal models and surgical procedures*

In order to ensure the results of the experiment as accurate as possible without being disturbed by other factors, researchers selected 12 female pigs weighing between 20 and 25 kg for the experiment. 3 full-thickness excisions (6 wounds totally on each individual animal) of about 5.0×5.0 cm were performed with sharp dissection on each side of dorsum, each wound was observed to have reached the level of subcutaneous deep fascia. Then different collagen scaffolds were applied and pressurized on the skin defects. The pigs were placed in separate cages after operation，and intramuscular Penicillin was applied on each subject for 3 days. All animals and experimental procedures used in this research were approved by the local Institutional Animal Care.

### *2.3 Evaluation of healing rate in porcine models*

72 wounds of 12 animals were divided into 3 groups: control group (Control, n=2×12), collagen group (Collagen, n=2×12), and Collagen/CBD-E7 peptide group (Collagen/CBD-E7 peptide, n=2×12). The wound area was photographed weekly by digital camera (Canon EOS 550D) at the first 4 weeks post surgery. The area of unhealed wound was measured based on the image using Photoshop software (Adobe Photoshop 7.0). Healing rate = [(original size - non-healing area)/original area] ×100% [13].

### *2.4 Analysis of cell infiltration*

At the first week after surgery, 3 subjects were sacrificed. A portion of wounds (1.0×1.0 cm) with normal tissues and collagen scaffolds at the margin were excised for cell infiltration observation. We evaluated the cellularization by counting cells infiltrated on the samples (hematoxylin eosin staining) in six random selected areas at 200× magnification level in a blinded fashion. The cells on the remained materials were obtained for cell enrichment analysis. After washing softly for three times, the remaining collagen was digested by collagenase type I. Then the cells were prepared for FACS ($CD45^-$ /$CD29^+$, $CD44^+$).

### *2.5 Histological observation*

At the 1w, 4w, 16w, 64w after operation, the wounds (1.0×1.0 cm) were excised at the margin contained the scaffolds and normal tissues. After fixed in 10% formalin, 5 mm paraffin sections were stained by hematoxylin eosin (HE, 1 w, 4 w, 16 w, 64 w), immunohistochemical (IHC, 1 w), masson trichrome (MT, 4 w, 64 w) and sirius red (SR, 16 w, 64 w) respectively for analysis of tissue vascularization, collagen formation and scar hyperplasia.

The capillaries were detected by immunostaining of anti-von Willebrand factor antibody (anti-vWF, 1:800, Abcam, USA) at 1 w. Two independent observers quantified the number of blood vessels for each section which was counted in six random selected areas at 200× magnification level in a blinded fashion.

MT and SR staining were used to evaluate the formation of collagen fibers. The presence and absence of collagen fibrillar structures within the wound bed was detected by MT staining. SR staining, considered to be one of the best understood techniques of collagen histochemistry, was use to assess the proportion between collagen type I and type III [14]. After dewaxed, serial sections were stained with hematoxylin for nuclei staining, and then stained by SR. Finally, the sections were observed under no-light environment polarizing light microscope (Nikon E400POLS, Japan)Image-Pro Plus 6.0 software was used for sirius red-positive analysis.

### *2.6 Statistical analysis*

Statistics were calculated with SPSS computer software for Windows (version 13.0, SPSS Inc, Chicago, IL). The data were expressed as means ± standard deviation (SD). Statistical differences between the groups were discerned by one-way analysis of variance (ANOVA). A probability value ($P$) of less than 0.05 was considered to be statistically significant. Statistically significant values were defined as $*P < 0.05$ and $**P < 0.01$.

## 3. Results

### *3.1. The collagen scaffold*

The collagen scaffold has widely interconnected pores which are suitable for cell infiltration, angiogenesis and nutrients diffusion (Fig. 1B). When conjugated with the CBD-E7 peptide, the interconnected pores of collagen scaffold were mostly filled.

At the  2nd week after surgery, the collagen scaffold was not fully absorbed, while at the 3rd week, the scaffold was almost invisible to human eye on the surface of wound.

### *3.2 Cellularization of collagen scaffolds in vivo*

At the first week after surgery, a greater number of cells were observed to have been raised in Collagen/CBD-E7 peptide group, while in Collagen group, the distributions of the cells were sporadic (Fig. 2A). The number of cells infiltrated in the implant in Collagen/CBD-E7 peptide group (400 ± 8.8) was significant higher than that of Collagen group (124 ± 9.9) (Fig. 2C). As analyzed by FACS, the proportion of cells ($CD45^-$ /$CD29^+$, $CD44^+$) enriched in Collagen/CBD-E7 peptide group (98.5% ±6.5) was significantly higher than that in Collagen group (76.3% ± 1.3) ( Fig. 2B).

### *3.3 Wound healing rate*

At the 1w after surgery, there was no great difference between the healing rates of the 3 groups as $P > 0.05$ (Fig. 3). Then a faster healing process of wounds was observed in Collagen/CBD-E7 peptide group at 2w, 3w, 4 w, with significant difference with other groups ($P < 0.05$, $P < 0.01$) (Fig. 3). In addition, the wound healing rate between Collagen group and Control group was also showed statistically significance ($P < 0.05$).

### *3.4 Vascularization induction by the Collagen/CBD-E7 peptide scaffold*

At the first week after surgery, the capillary density of Collagen / CBD-E7 peptide group (79.69 ± 8.25) in wound granulation tissue was significantly higher than that of Collagen group (57.84 ± 4.96) and Control group (36.62 ± 6.43) (Figure 4B & C), which is fin accordance with the evidence provided by HE staining (Figure 4A).

### *3.5 Collagen determination and scar assessment in wound area*

The type and morphology of collagen fibers are considered to be the key of scar formation [15], which can be observed by applying HE, MT and SR staining in order to analyze the collagen type and study the distribution in regenerated tissues.

At the 4w and the 64w, the arrangement of collagen fibers in the wound was observed by applying HE and MT staining. As showed in Fig. 5 and Fig. 8, the collagen fibers in Collagen/CBD-E7 peptide group were orderly arranged. They paralleled to the epidermis in the upper layer, and reticulated in the lower layer. While in Collagen and Control group, the thick fibers were randomly and messily arranged.

At the 16w and the 64w after surgery, the fiber type of regenerated skin was evaluated by SR staining, where the red area denoted collagen type I and green denoted collagen type III. Type I collage fibers arrayed lightly, indicating a strong bilateral refraction and yellow, orange, and red thick fibers. Type □ collagen fibers arrayed like a dispersed net, indicating a weak bilateral refraction and green thin fiber. As shown in Fig. 6B and Table 1, the proportion of collagen type III was more than collagen type I in

Collagen/CBD-E7 peptide group at the 16w. However, the ratio between collagen type I and collagen type III reached natural skin tissue balance at the 64w(Fig.8 C and Table 1).

**Table 1** –The proportion of collagen type I to type III in different groups at 16w and 64w.

| | | | | | | |
|---|---|---|---|---|---|---|
| Time Point | | 16w | | 64w | | |
| Group | n | type III % | I/III | type III % | I/III | |
| Control | 6 | 12% | 7.42:1 | 5% | 9.46:1 | |
| Collagen | 6 | 19% | 4.29:1 | 14% | 6.02:1 | 2.17:1 |
| Collagen/CBD-E7 peptide | 6 | 34% | 1.93:1 | 32% | | |

### *3.6 Re-growth of skin appendages in wound area*

At the 16w after surgery, the regeneration of cutaneous appendages was observed. Hair follicle cells were found in Collagen/CBD-E7 peptide group, while no skin appendages was observed in Collagen and Control group. Fig. 7 showed the formation of Hair follicle in Collagen/CBD-E7 peptide group.

We continued to study the regeneration of cutaneous appendages at the 64w. The sudoriferous gland and hair follicle were found in the regenerated skin (Fig. 9).

## 4. Discussion

Wound repair is a complex biological process that requires the synergy of multiple cell types and physiological processes[16]. The biological responses to such process can be divided into three categories: inflammation, proliferation and remodeling. In previous study the application of exogenous cytokines (e.g. VEGF, bFGF, HGF) for the treatment of tissue defects has been highlighted. However, exogenous cytokines are susceptible to metabolic loss by the inflammatory exudate's scouring effect [13]. Furthermore, wound repair is a dynamic multistep process stimulated by interaction of multiple factors, including growth factors, extracellular matrix, microenvironment and individual differences. Therefore, the cytokines alone can partially accelerate the regenerated process. In the meanwhile ,there is uncertainty as to whether cytokines improve regulating the whole complex process[17]. In this study, we demonstrate that the functional scaffold could recruit MSCs specifically *in vivo*, it also helps accelerate the healing process and promote the regeneration of cutaneous appendages.

At the first week after surgery, the cell number in the material reflected the early tendency of cell migration and the biocompatibility of the scaffold (Fig. 2A), from which we infer that CBD-E7 peptide is capable of enhancing the recruitment of stem cells to scaffold and the scaffold may provide a proper environment for cell survival and subsequent cascading response to injury. It is well known that the neovascularization

is an essential step in the complex wound healing process [4]. Compared to Collagen group at the first week (1w) (Fig. 2 and Fig. 4), we found more cells and capillaries in Collagen/CBD-E7 peptide group. There is already evidence that the infiltration and migration of cells, especially endothelial cells, are necessary for angiogenesis [18]. Some of the endothelial cells or hematopoietic stem cells could also be enriched at the target site, which increased the blood vessel formation around the wound and improved the blood perfusion, thereby accelerated the wound healing process.

In this study, we hypothesized that due to the CBD-E7 peptide immobilized on scaffold, the MSCs around the injury sites could migrate to the scaffold, and then exert their capability of multi-lineage differentiation. Moreover, the reason why collagen scaffold emerged to be one of the most functional biomaterials is also because of its excellent biocompatibility and biodegradability, which are also important for the survival of stem cells, might facilitate cell-scaffold interactions including migration, proliferation and differentiation [13].

There are opinions that claim the CBD technology has the advantage of both perdurability and specificity. [13] As described by Zhang J. etc. [19], the collagen-binding domain (CBD) could bind to collagen I specifically and recombine with protein or cytokines. When applied in injury study, the synthetic protein could release active substance sustainably and slowly [14]. In this study, the collagen scaffold binding with specific MSCs affinity E7 peptide could capture autologous MSCs to accelerate the healing progress. It is generally acknowledged MSCs have been identified as CD29 positive, CD44 positive and CD45 negative [5, 20]. In this study, adhered cells on scaffolds were characterized as mesenchymal stem cells ($CD45^-$ /$CD29^+$, $CD44^+$) which were verified by FACS.

Although Skin scars indicate the completion of mammalian tissue repair, they are considered detrimental to the functional recovery of tissues. They can cause unpleasant symptoms such as severe itching, tenderness, pain, anxiety, depression or even disruption of daily activities [11]. However, scar was often neglected in wound healing studies [21]. In general, wounds that have not healed within 3-4 weeks are considered to have great risk of excessive scar formation [22]. The healing rate in Collagen/CBD-E7 peptide group was significant higher than other groups at the 2nd, 3rd and 4th week. At the 4 w after operation, the defect was already cured in Collagen/CBD-E7 peptide group. And at the 16 w, the wound in Collagen/CBD-E7 peptide group presented as a linear scar, while in Control group the scar turned dull-red and raised (Fig. 6A).

The severity of scars is usually judged by naked human eye, but it can be assessed quantitatively with SR-positive analysis by Image-Pro Plus 6.0 software. Proper proportion of type I and III collagen is essential for healing quality. In this study, we found that during the formation of scar, the proportion of collagen type I increased while collagen type III descended. The changes of ratio on collagen type I to type III would lead to abnormal biological behaviors. In tissues with great elasticity, collagen type III (thin fibers) was much more than collagen type I, with a lower degree of fibrosis. As shown in Fig. 6 and Table 1, the proportion of collagen type III in Collagen/CBD-E7 peptide group was much higher than other

groups at 16 w, which indicated a better healing quality. While at the 64 w, the ratio of collagen type I/III was similar to normal tissues and the appearance and intensity of scars decreased.

Mammalian skin is a complex structure that consists of the epidermis, dermis, and the epidermal appendages, with the epidermis and dermis separated by a basement membrane [23]. An ideal wound healing is described as a completely regeneration with full functional recovery that has no difference from the original uninjured skin [11]. Generally speaking, patients with severe burns or large defects usually have problems brought by scars such as sweat insufficiently or partial loss of hair. At the 16 w after the operation, the hair follicle was found in Collagen/CBD-E7 peptide group. We can infer that the functional collagen scaffold may have a long-term effect in full-thickness skin defect. And at the 64 w, it was exciting that we found the cutaneous appendages include sudoriferous gland and hair follicle in regenerated skin.

Scar-free skin healing exists in the early stages of mammalian embryos, but it gradually turns to scar healing as the embryos develops [16]. H. Peter Lorenz. etc. [23] believe that MSCs from multiple sources contribute to scarless fetal wound healing. We believe that the mesenchymal stem cells recruited to the functional scaffold could promote the regeneration of skin and prevent scar formation simultaneously.

In summary, these data provided new insights for the treatment of acute full-thickness skin wounds by cellular-material therapy and should contribute to new strategies for the treatment of chronic wounds and scar intervention.

# Conclusions

In this work, the collagen scaffolds functionalized with the specific MSCs affinity peptide were experimented in porcine wound healing models. After implantation on the injured skin, the functional scaffold could effectively enhance the recruitment of MSCs to local wound site, accelerating the healing progress and promote the regeneration of cutaneous appendages. This study provided new insights for enriching autologous stem cells to the wound site and contributed to new methods for the treatment of wound healing with less scar formation.

# Declarations


### Acknowledgments

This work was supported by grants from National Natural Science Foundation of China (81272108 and 31300806), Key Project of Nanjing Bureau of Health (ZKX13024), Project of Nanjing Science and Technology Development (201201069).


# References

1. Proksch E, Brandner JM, Jensen J-M. The skin: an indispensable barrier. Experimental Dermatology 2008;17:1063-72.
2. Clark RA, Ghosh K, Tonnesen MG. Tissue engineering for cutaneous wounds. The Journal of investigative dermatology 2007;127:1018-29.
3. Ma K, Liao S, He L, Lu J, Ramakrishna S, Chan CK. Effects of Nanofiber/Stem Cell Composite on Wound Healing in Acute Full-Thickness Skin Wounds. Tissue Engineering Part A 2011;17:1413-24.
4. Jiang Y, Chen B, Liu Y, Zhufu Z, Yan X, Hou X, et al. Effect of Collagen Scaffold with Adipose-derived Stromal Vascular Fraction Cells on Diabetic Wound Healing: A Study in a Diabetic Porcine Model. Tissue Engineering and Regenerative Medicine 2013;10:192-9.
5. Yagi H, Soto-Gutierrez A, Parekkadan B, Kitagawa Y, Tompkins RG, Kobayashi N, et al. Mesenchymal Stem Cells: Mechanisms of Immunomodulation and Homing. Cell Transplantation 2010;19:667-79.
6. Motegi SI, Ishikawa O. Mesenchymal stem cells: The roles and functions in cutaneous wound healing and tumor growth. Journal of dermatological science 2016.
7. Shao Z, Zhang X, Pi Y, Wang X, Jia Z, Zhu J, et al. Polycaprolactone electrospun mesh conjugated with an MSC affinity peptide for MSC homing in vivo. Biomaterials 2012;33:3375-87.
8. Falanga V, Iwamoto S, Chartier M, Yufit T, Butmarc J, Kouttab N, et al. Autologous bone marrow-derived cultured mesenchymal stem cells delivered in a fibrin spray accelerate healing in murine and human cutaneous wounds. Tissue Engineering 2007;13:1299-312.
9. Borena BM, Pawde AM, Amarpal, Aithal HP, Kinjavdekar P, Singh R, et al. Evaluation of autologous bone marrow-derived nucleated cells for healing of full-thickness skin wounds in rabbits. International Wound Journal 2010;7:249-60.
10. Wang H, Yan X, Shen L, Li S, Lin Y, Wang S, et al. Acceleration of wound healing in acute full-thickness skin wounds using a collagen-binding peptide with an affinity for MSCs. Burns & trauma 2014;2:181-6.
11. Bayat A, McGrouther DA, Ferguson MWJ. Skin scarring. British Medical Journal 2003;326:88-92.
12. Shi C, Li Q, Zhao Y, Chen W, Chen B, Xiao Z, et al. Stem-cell-capturing collagen scaffold promotes cardiac tissue regeneration. Biomaterials 2011;32:2508-15.
13. Yan X, Chen B, Lin Y, Li Y, Xiao Z, Hou X, et al. Acceleration of diabetic wound healing by collagen-binding vascular endothelial growth factor in diabetic rat model. Diabetes Research and Clinical Practice 2010;90:66-72.
14. Tan Q, Chen B, Yan X, Lin Y, Xiao Z, Hou X, et al. Promotion of diabetic wound healing by collagen scaffold with collagen-binding vascular endothelial growth factor in a diabetic rat model. Journal of Tissue Engineering and Regenerative Medicine 2014;8:195-201.
15. Hardy MA. The biology of scar formation. Physical therapy 1989;69:1014-24.
16. Le Provost GS, Pullar CE. beta 2-Adrenoceptor Activation Modulates Skin Wound Healing Processes to Reduce Scarring. Journal of Investigative Dermatology 2015;135:279-88.

17. He Q, Zhao Y, Chen B, Xiao Z, Zhang J, Chen L, et al. Improved cellularization and angiogenesis using collagen scaffolds chemically conjugated with vascular endothelial growth factor. Acta Biomaterialia 2011;7:1084-93.
18. Wang LS, Li L, Shojaei F, Levac K, Cerdan C, Menendez P, et al. Endothelial and hematopoietic cell fate of human embryonic stem cells originates from primitive endothelium with hemangioblastic properties. Immunity 2004;21:31-41.
19. Zhang J, Ding L, Zhao Y, Sun W, Chen B, Lin H, et al. Collagen-Targeting Vascular Endothelial Growth Factor Improves Cardiac Performance After Myocardial Infarction. Circulation 2009;119:1776-84.
20. Rankin S. Mesenchymal stem cells. Thorax 2012;67:565-6.
21. Soller EC, Tzeranis DS, Miu K, So PTC, Yannas IV. Common features of optimal collagen scaffolds that disrupt wound contraction and enhance regeneration both in peripheral nerves and in skin. Biomaterials 2012;33:4783-91.
22. Brusselaers N, Pirayesh A, Hoeksema H, Verbelen J, Blot S, Monstrey S. Burn scar assessment: a systematic review of different scar scales. The Journal of surgical research 2010;164:e115-23.
23. Hu MS, Rennert RC, McArdle A, Chung MT, Walmsley GG, Longaker MT, et al. The Role of Stem Cells During Scarless Skin Wound Healing. Adv Wound Care (New Rochelle) 2014;3:304-14.

# Figures

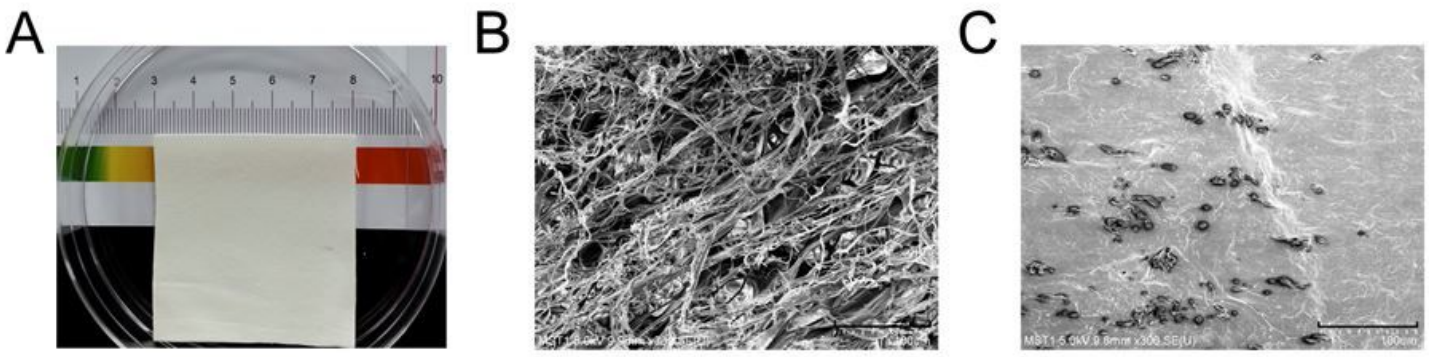


**Figure 1**

The CBD-E7 functional collagen scaffolds. A. Macrograph of the collagen scaffold; B. SEM image of the collagen scaffold pre-treatment. Scale bar =100 μm; C. SEM image of the collagen scaffold post-treatment. Scale bar =100 μm.

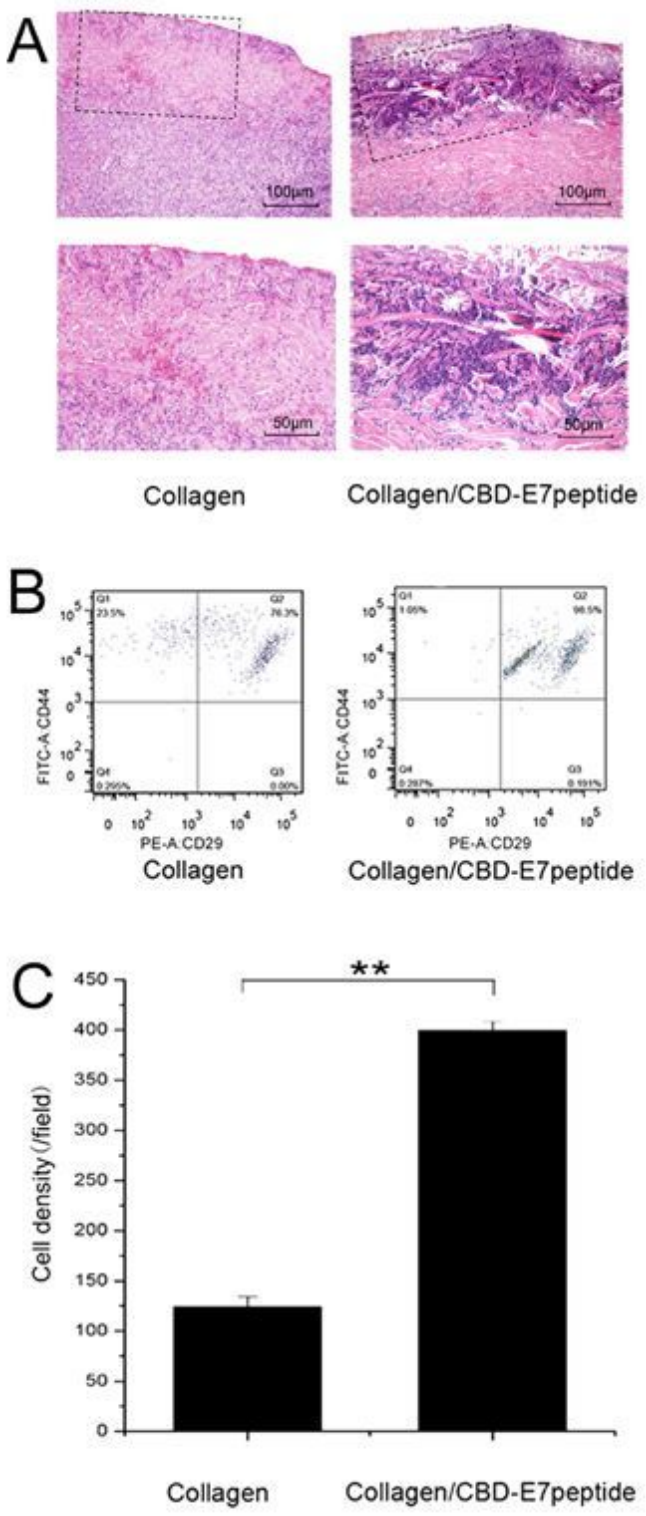


## Figure 2

Analysis of cellularization on collagen scaffolds. A. Cells infiltrated on Collagen group and Collagen/CBD-E7 peptide group at 1w after surgery (Top, scale bar = 100 μm) and the amplified images of the black frames (Bottom, scale bar = 50 μm); B. Analysis of the cells remained on the implant by FACS; C. Statistical analysis of cell density between Collagen group and Collagen/CBD-E7 peptide group at 1w.

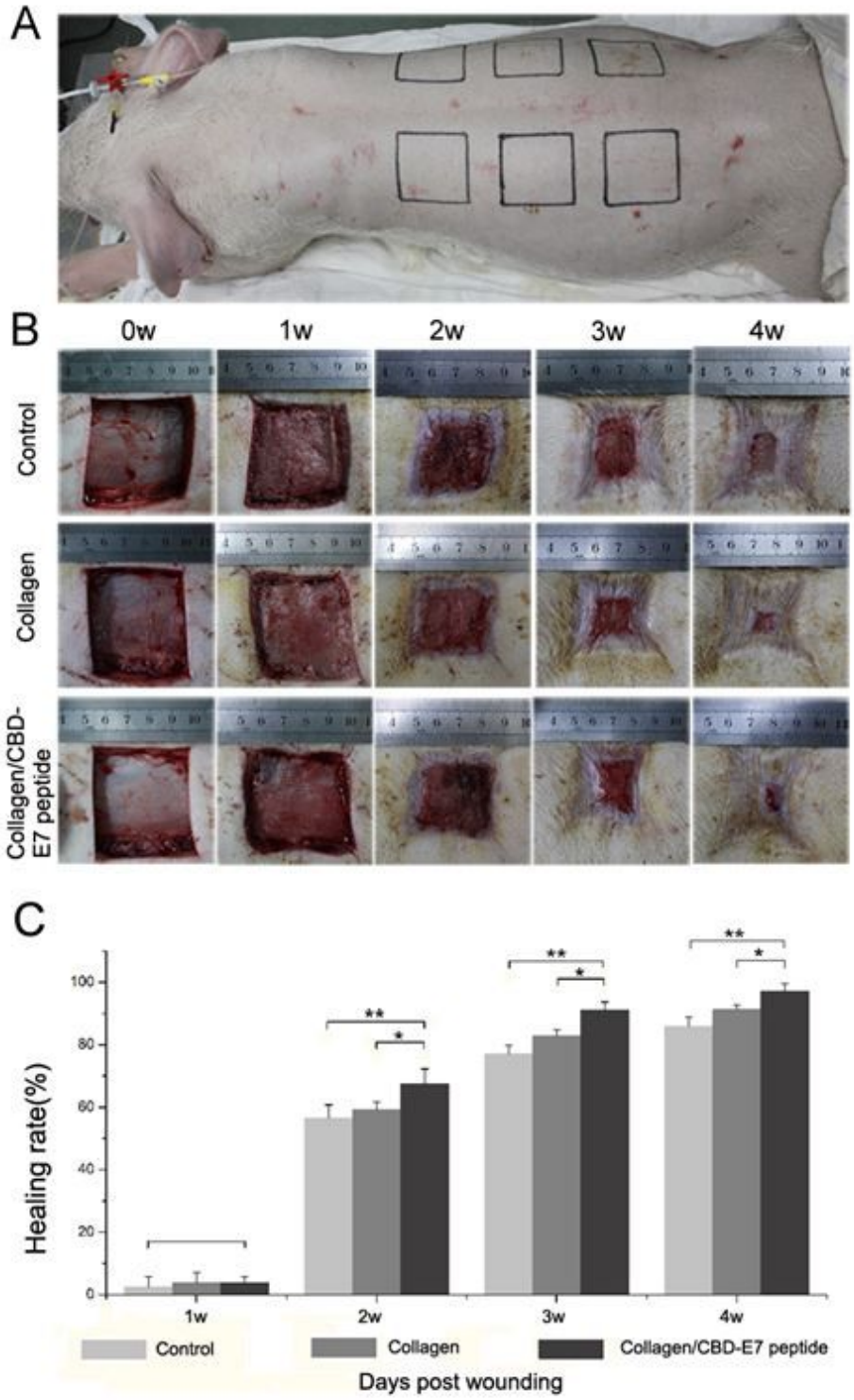


## Figure 3

The observation of wound healing rate. A. The diagram of porcine wound models; B. Appearances of wounds in different groups at 0 w, 1 w, 2 w, 3 w and 4 w; C, The statistical analysis of healing rate in different groups. 1 w: Collagen/CBD-E7 peptide: 3.86 ± 1.8%, Collagen: 3.09 ± 3.1%, Control: 2.48 ± 2.9%; 2 w: Collagen/CBD-E7 peptide 67.46 ± 4.8%Collagen59.13 ± 2.6%Control56.58 ± 4.1%3 w: Collagen/CBD-E7 peptide 91.10 ± 2.6%Collagen82.95 ± 1.9%Control76.99 ± 2.9%4 w:

Collagen/CBD-E7 peptide 97.11± 2.4%Collagen91.19 ± 1.5%Control85.79 ± 3.1%. Data are presented as mean ± SD. **P < 0.01, *P < 0.05.

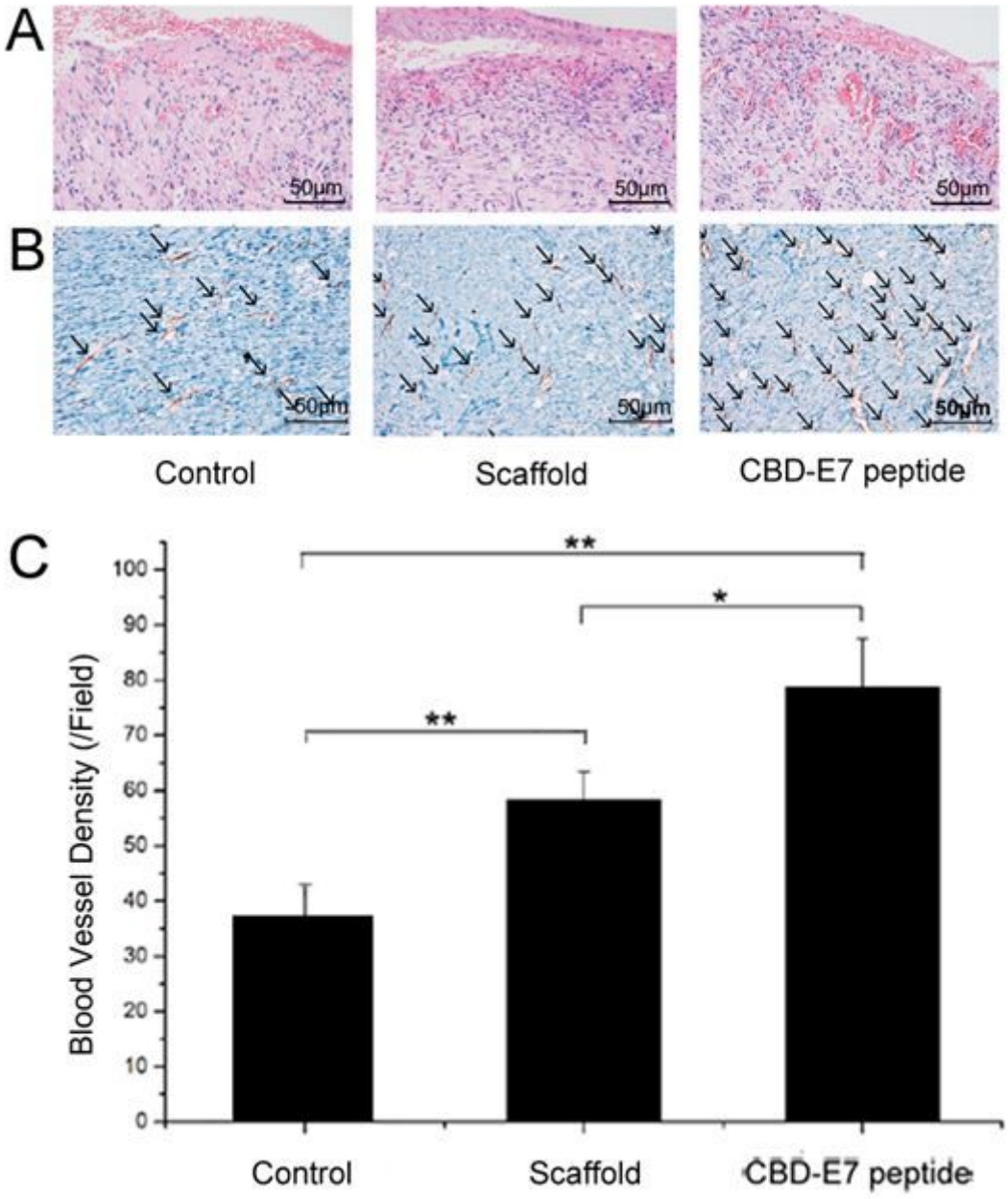


## Figure 4

Analysis of vascularization in skin wounds at 1 w after surgery. A. HE staining in the wound granulation tissues; B. IHC staining for capillary vessel. Arrows point to blood vessels; C. Statistical analysis of the blood vessel density. Data are presented as mean ± SD**P < 0.01.

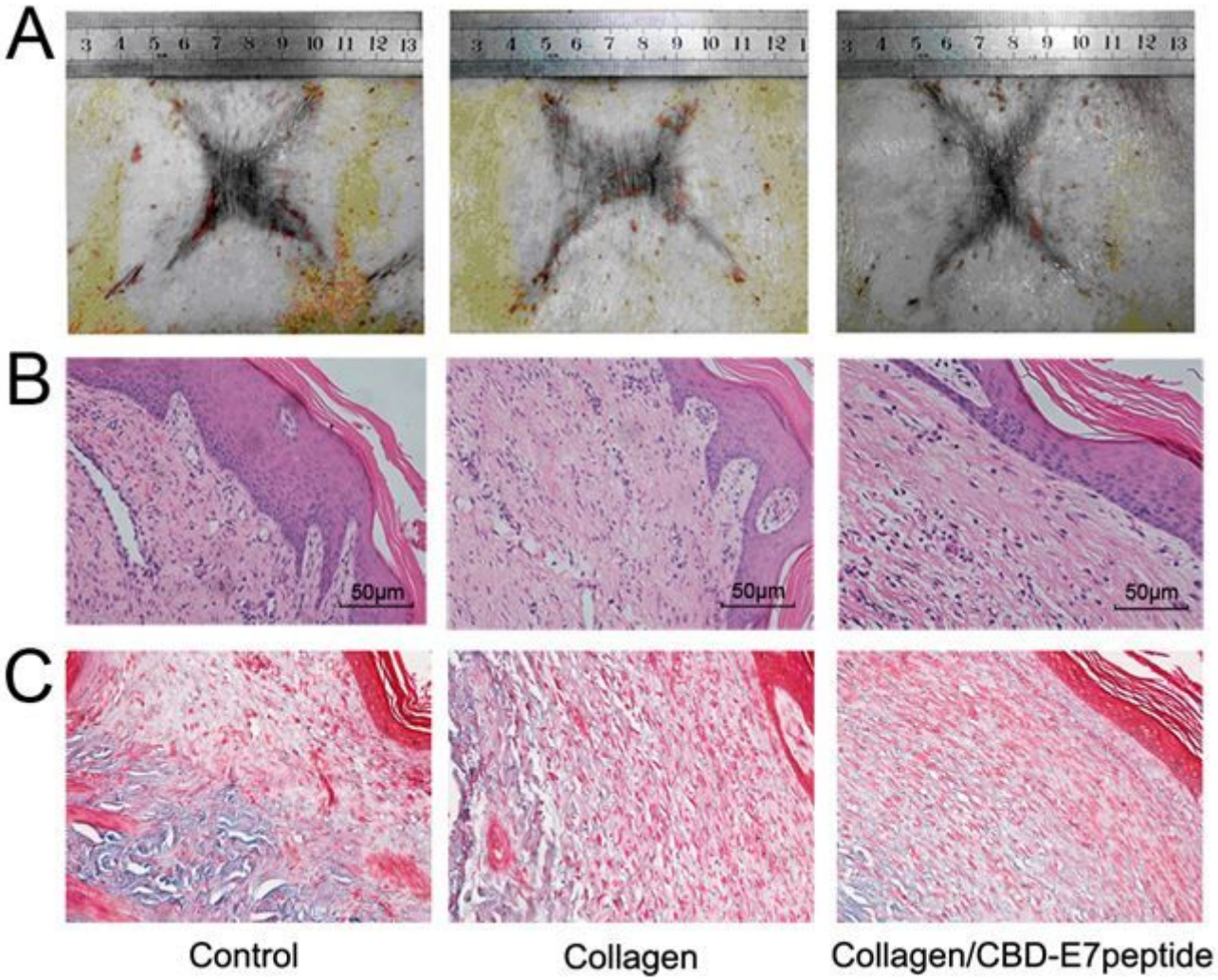


## Figure 5

A. Overview of the skin wounds at 4 w; B. HE staining for collagen fibers; C. MT staining for detecting the presence (green) and absence (red) of collagen fibrillar structures within the wound bed.

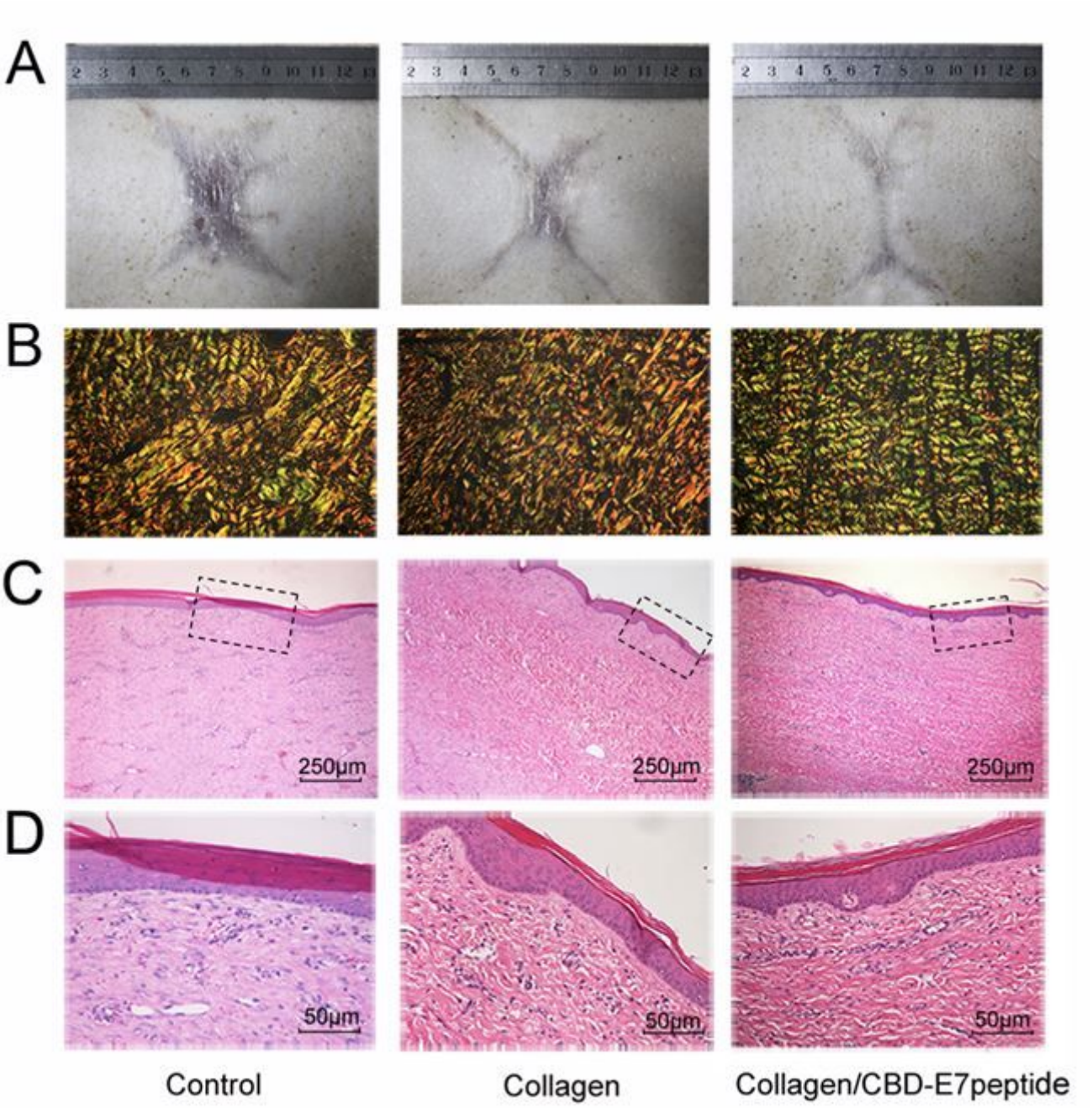


## Figure 6

Overview images, SR and HE staining of the skin wounds at 16w. A. Overview of the skin wounds; B. SR staining for collagen type. The red area denotes collagen type I and green denotes collagen type III; C. HE staining of the skin wounds. Scale bar = 250 μm; D. The amplified images of HE staining, Scale bar = 50 μm.

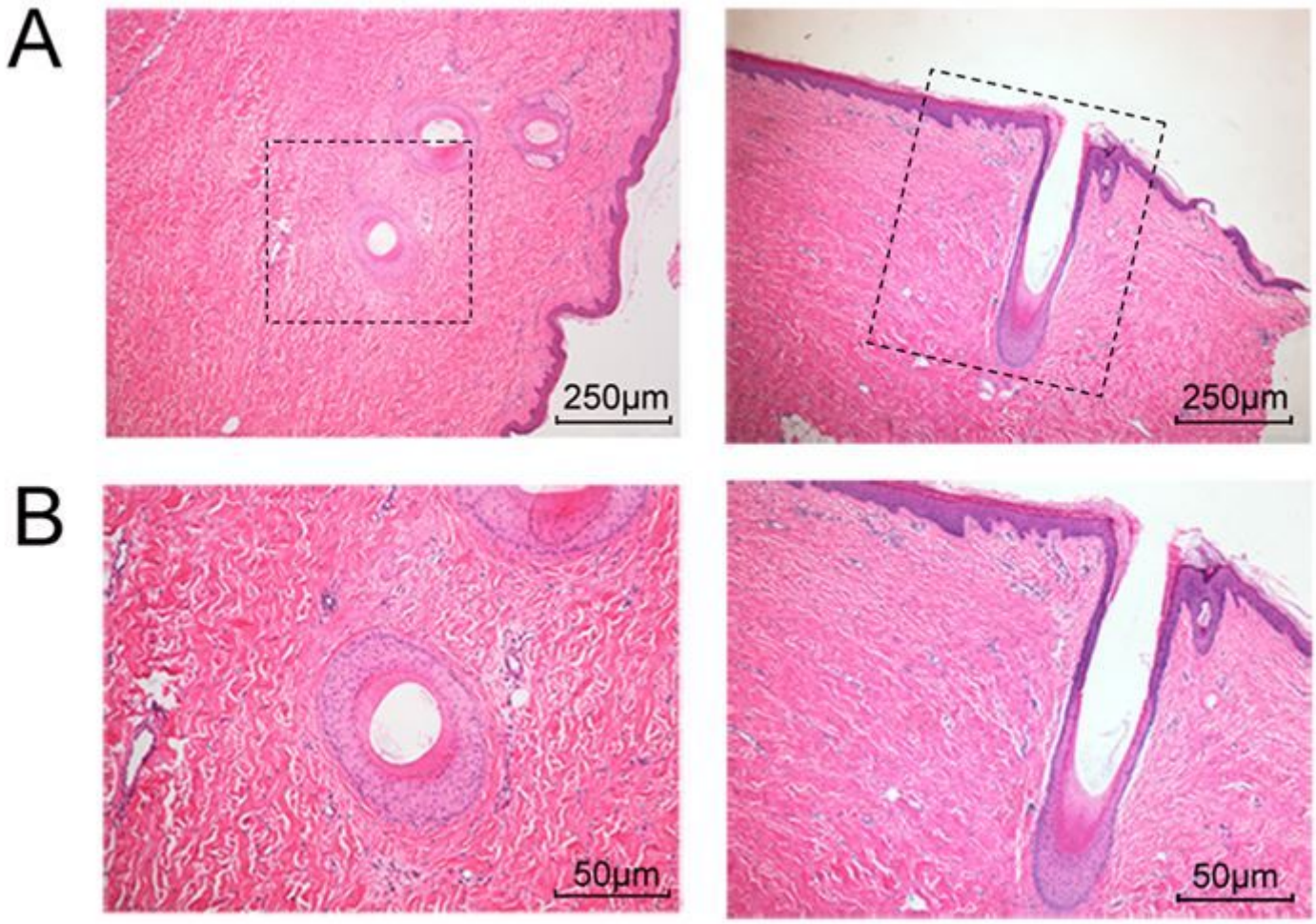


**Figure 7**

Re-growth of Hair follicle in Collagen/CBD-E7 peptide group by HE staining at 16 w. A. HE staining of the Hair follicle cell (transverse and longitudinal section). Scale bar = 250 μm; B. The amplified images of the black frames of A, Scale bar = 50 μm.

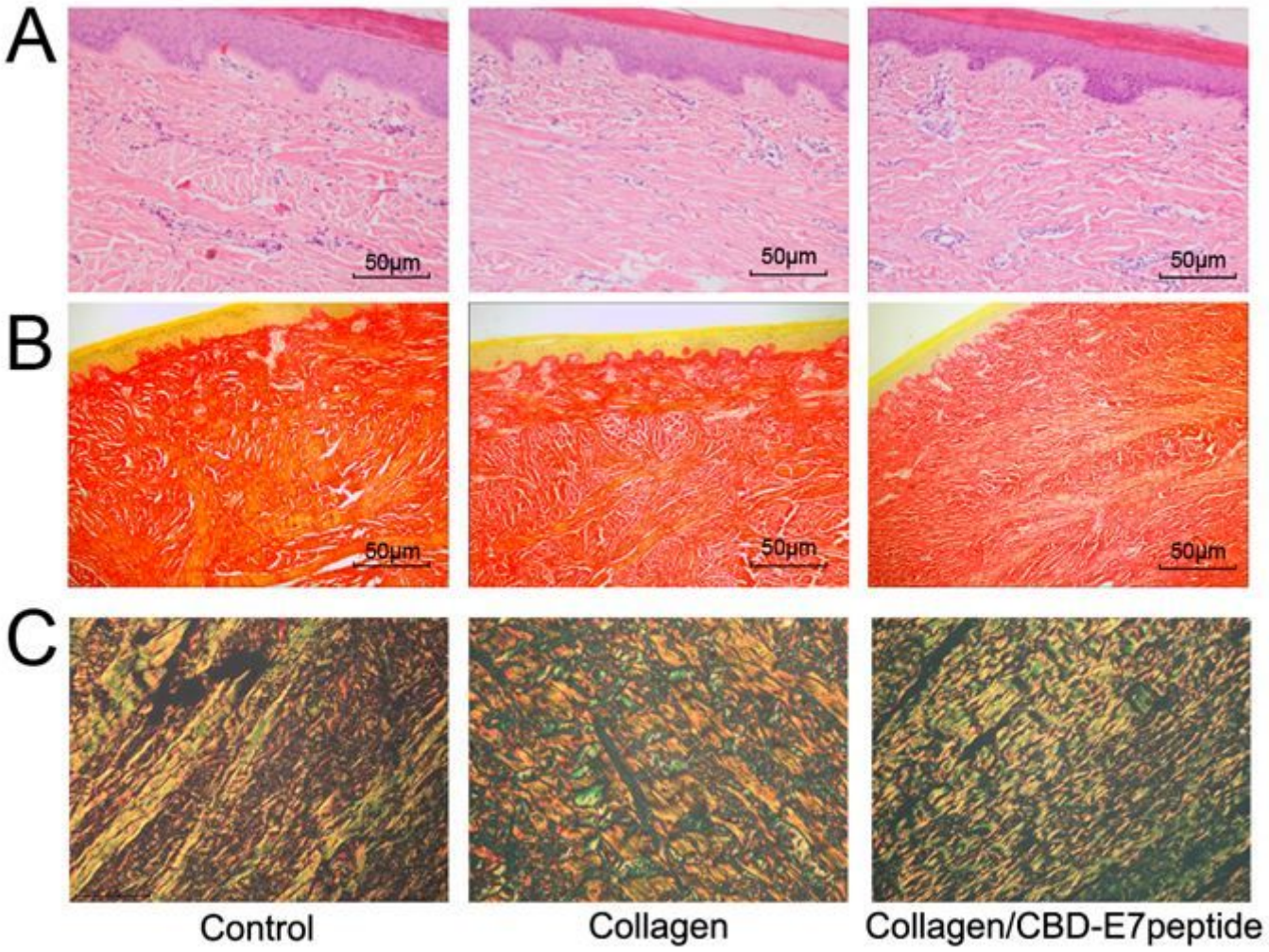


## Figure 8

HE, MT and SR staining of the wounds at 64 w. A. HE staining of the skin wounds. Scale bar = 50 μm; B. MT staining of the skin wounds. Scale bar = 50 μm; C. SR staining of the skin wounds.

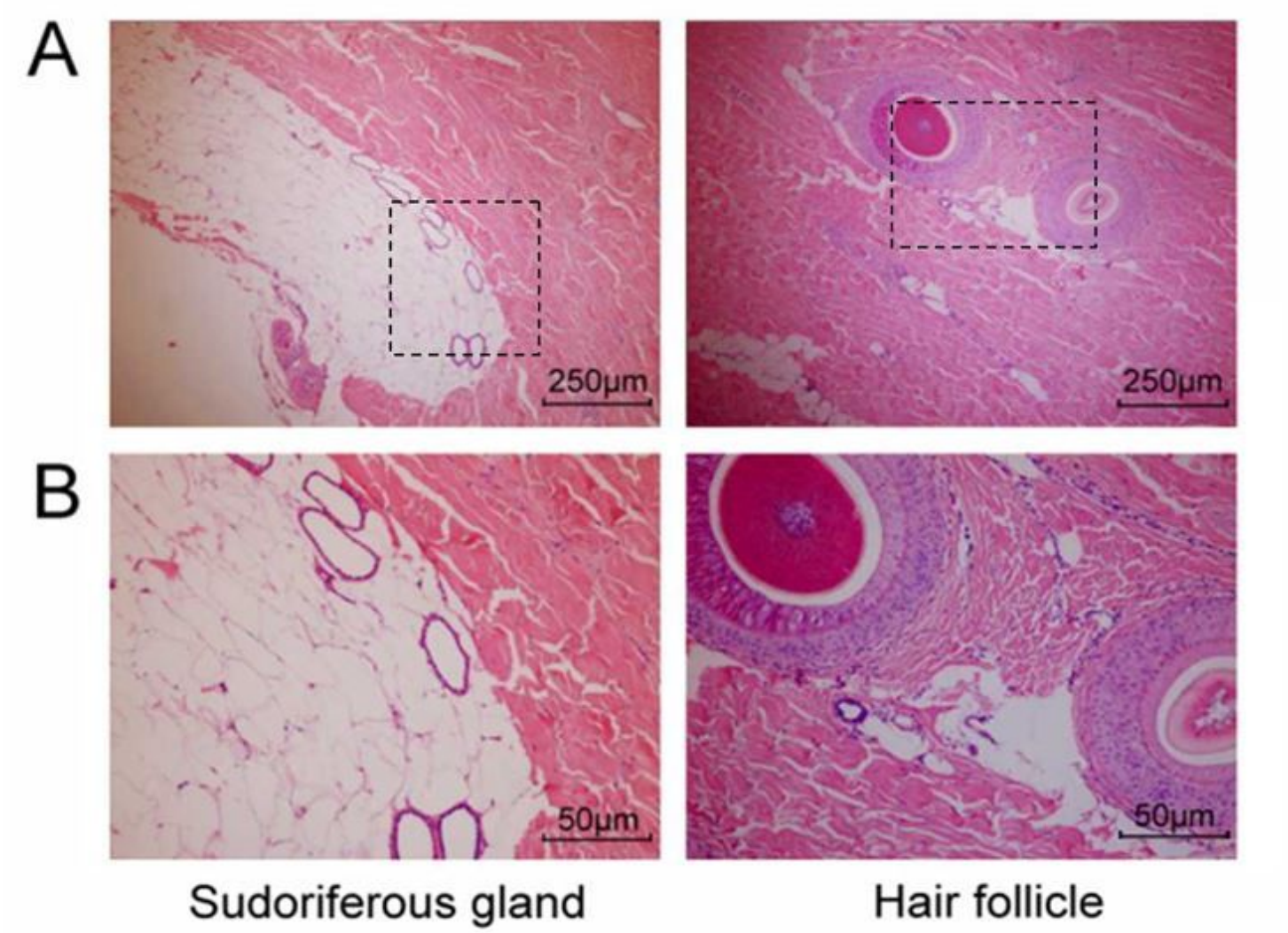


**Figure 9**

Re-growth of sudoriferous gland and hair follicle in Collagen/CBD-E7 peptide group by HE staining at 64 w. A. HE staining of the sudoriferous gland (left) and hair follicle (right). Scale bar = 250 μm; B. The amplified images of the black frames fields of A. Scale bar = 50 μm.